Theory of carriers bound to In isoelectronic δ-doping layers in GaAs

M. Di Ventra
Institut de Physique Appliquée-Laboratoire de Théorie du Solide, Ecole Polytechnique, Fédérale de Lausanne, PHB-Ecublens, CH-1015, Lausanne, Switzerland

K. A. Mäder
Centre Européen de Calcul Atomique et Moléculaire, ENS-Lyon, 69364 Lyon cedex 07, France
(Received 10 October 1996; revised manuscript received 12 December 1996)

We present a model for ultrathin InAs impurity interlayers embedded in bulk GaAs. It is based on an empirical tight-binding Green's function scheme with basis functions that are Bloch-like in the in-plane direction and Wannier-like perpendicular to it. Spin-orbit interaction and strain are consistently included. Our results are in good agreement with recent experimental data as far as the heavy-hole − electron transition is concerned. Conversely, our calculations indicate that one layer of InAs in bulk GaAs induces a light-hole state degenerate with the continuum 3 meV below the GaAs valence-band edge. This is in contrast with effective-mass calculations that predict a type-I light-hole configuration in this system. The importance of strain in leading to this energy-level configuration is stressed. We suggest that absorption or temperature-dependent luminescence experiments could distinguish between a bound or an unbound light-hole state. [S0163-1829(97)00819-9]

I. INTRODUCTION

Experimental investigation of the optical properties of very thin (less than 30 Å) layers of impurity atoms embedded in bulk host materials has considerably increased in recent years due to significant progress in growth technology.[1–8] The controlled growth of such interlayers has allowed us to observe pronounced radiative recombination processes without phonon participation even in indirect-gap materials.[7] The reason for this lies in the recombination efficiency of gap states confined to the impurity layer, which are bound by the short-range potential describing the impurity substitution (''δ layer,'' or ''quantum well'').

From a theoretical point of view, less effort has been devoted to the study of such structures on a *microscopic* level. Size and computing time limitations force state-of-the-art self-consistent calculations to use rather small supercells with periodic boundary conditions. For example, in a recent simulation of isolated InAs monolayers in GaAs, an eight-monolayer periodic supercell was employed.[9] Much larger supercells, with virtually quenched finite-size effects, can be employed in non-self-consistent, empirical pseudopotential calculations, as it has been demonstrated for AlAs/GaAs quantum structures.[10,11] *Macroscopic* models, which average the electron potential over one or several crystal unit cells, such as the envelope-function approximation (EFA), are, in principle, inadequate to describe the electronic properties of atomic-scale, thin δ layers.

An atomic-scale study of such systems is thus in order, which takes into account all band-structure features of the host and perturbing materials. Some models in this direction have employed an empirical tight-binding (ETB) scheme.[12–14] Recently, an ETB model has been applied successfully by the present authors to explain some experimental results on very thin InAs layers in bulk InP.[15]

The ETB model is suitable for this kind of problems for two main reasons. (i) the only input parameters are some band-structure values of the host and substitution *bulk* materials which can be inferred from experiment or from empirical and *ab initio* model calculations and are sufficient to reproduce the band dispersions throughout the Brillouin zone. (ii) The ETB is an atomistic model and makes no assumption on the wave-functions shape and on their interface matching conditions.

The object of this paper is to study in detail the electronic properties of one monolayer (ML) of InAs in bulk (001) GaAs following the ETB model proposed in Ref. 14. Simple considerations on the competing values of the misfit dislocation energy and the elastic misfit strain energy show that 1 ML represents the growth limit for pseudomorphic InAs on GaAs substrate[16] even if very recent measurements by Patanè *et al.* show the absence of a critical thickness for the self-aggregation of quantum dots in these systems.[17]

A single, isoelectronic In_{Ga} impurity in GaAs does not induce any level in the gap of the latter. Conversely, it has been demonstrated[1–7] that one nominal sheet of In atoms in GaAs shows luminescence peaks at energies corresponding to levels in the GaAs gap. The interpretation of such peaks, especially those corresponding presumably to the light-hole (LH) state, is not yet fully settled down. Thus, a complete, three-dimensional theory of the electronic structure has to be established that describes at a high level of accuracy the conduction-band (CB) as well as the valence-band states and goes beyond the EFA picture of parabolic band dispersions and one-dimensional Kronig-Penney potentials.

The paper is organized as follows. In Sec. II we describe the present ETB model. In Sec. III we discuss the results. The Appendix contains some details about the inclusion of spin-orbit interaction and strain in our ETB model.

II. THEORY

Our approach is based on a Koster-Slater model for short-range impurity potentials in an infinite host lattice.[18] In contrast to other more recent applications of the Koster- Slater model to isovalent impurity layers in semiconductors,[12,13] (i) we consider valence and conduction bands simultaneously, (ii) we do not constrain the impurity potential to one given symmetry (e.g., *s* like) or to be on-site only, and (iii) we include both spin-orbit and strain contributions to the electron Hamiltonian. In our model, the symmetry and range of the impurity-layer potential are consistent with the atomic geometry of the interlayer and the atomiclike basis set and range of interactions retained in the empirical tight-binding Hamiltonian of the *host material*. We describe the host crystal by an ETB Hamiltonian H^0 in a basis of sp^3s^* atomic like orthogonal orbitals centered on each atomic site.[19] We retained only nearest-neighbor interactions that are sufficient to reproduce the valence-band and the lower conduction-band dispersions even of indirect-gap materials.[20] In-plane atomic positions have been fixed to the zinc-blende GaAs lattice, which corresponds to pseudomorphic growth conditions. The interplane distances between the In and As atoms have been chosen to be equal to those predicted by the macroscopic theory of elasticity for a lattice mismatch between InAs and GaAs of 7.2%. This ansatz is supported by recent *ab initio* calculations[9] and experimental x-ray measurements[21] on this system which show no breakdown of the continuum elasticity theory in predicting the interplane distortion even in the ML limit.

The perturbation matrix $U=H-H^0$, to be added to H^0 in order to construct the total Hamiltonian H describing the impurity system, is calculated by taking the difference between the ETB parameters of the completely substituted system, i.e., *strained* bulk InAs, and those of the host, i.e., bulk GaAs. This procedure is obviously ''exact'' for infinite δ-layer thickness, where interface effects are unimportant. For finite layer thickness, however, and in particular for very thin interlayers, interface effects are important and cannot simply be parametrized in terms of bulk properties alone. We adopt the following heuristic model: Instead of abruptly ''switching'' from host to impurity parameters at some *arbitrary interface boundary of zero width*, we scale the on-site impurity matrix elements by a factor 1/2 at the *common-ion (As) boundary layer*. A similar idea has proven to be very reliable for a variety of AlAs/GaAs structures in the context of empirical (screened) atomic pseudopotentials.[10] Moreover, in order to account for the strain effects on the electronic states in the present lattice-mismatched case, the InAs ETB parameters have been carefully fitted to reproduce the relevant deformation potentials (see the Appendix). In Table I we report the parameters used in this calculation for the GaAs and for the InAs *pseudomorphically strained* on GaAs. The notation is the same as in Ref. 19. Further details and technicalities of the present ETB approach are summarized in the Appendix.

Since the model is not self-consistent we rigidly shift the on-site matrix elements of U by an amount $\Delta\overline{E_v}=0.04$ eV, which is the average band offset between the strain and spin-orbit split valence-band maxima of the two materials. Its value has been taken from Ref. 22. The zero of energy is positioned at the valence-band maximum of GaAs.

TABLE I. Parameters for GaAs and InAs strained on GaAs used in the ETB calculation. The notation is the same as in Ref. 19. All energies are in eV. λ_a and λ_c are the spin-orbit parameters introduced by Chadi (Ref. 31).

Parameters	GaAs	InAs
$E(s,a)$	-8.3580	-9.5381
$E(p,a)_{x,y}$	0.9285	0.6757
$E(p,a)_z$	0.9285	0.9685
$E(s^*,a)$	7.4283	7.2724
$E(s,c)$	-2.6718	-2.7223
$E(p,c)_{x,y}$	3.5558	3.4858
$E(p,c)_z$	3.5558	3.7786
$E(s^*,c)$	6.6268	6.6090
V_{ss}	-6.4349	-5.9828
$V_{xx,yy}$	1.9548	1.4677
V_{zz}	1.9548	2.7912
V_{xy}	5.0234	4.1215
$V_{xz,yz}$	5.0234	4.7372
$V(sa,pc)_{x,y}$	4.4390	2.9784
$V(sa,pc)_z$	4.4390	3.4234
$V(sc,pa)_{x,y}$	5.7320	5.3143
$V(sc,pa)_z$	5.7320	6.1083
$V(s^*a,pc)_{x,y}$	4.2981	3.1742
$V(s^*a,pc)_z$	4.2981	3.6485
$V(s^*c,pa)_{x,y}$	4.6327	3.6715
$V(s^*c,pa)_z$	4.6327	4.2200
λ_a	0.1300	0.0242
λ_c	0.0540	0.1428

All relevant quantities such as the density of states (DOS), bound-state and resonant-state energies, and wave functions are calculated in the Green's-function formalism. In order to exploit the short-range nature of the isoelectronic impurity layer perpendicular to the layer plane, we represent the Green's-function matrix of the host material G^0 in a basis that is Bloch-like in the plane parallel to the impurity layer and Wannier-like perpendicular to it.[12] It is related to the ETB atomiclike basis by a unitary transformation and can be written as

$$|l\mathbf{K}j\rangle=\frac{1}{\sqrt{N_\perp}}\sum_{\mathbf{k}_\perp} e^{-i\mathbf{k}_\perp\cdot\mathbf{R}_j}|l,\mathbf{K}+\mathbf{k}_\perp\rangle, \tag{1}$$

where $l=s,p_x,p_y,p_z,s^*$; $\mathbf{K}$ is a two-dimensional wave vector lying in the (001) plane; j indexes the layers; $\mathbf{R}_j$ is any lattice vector of layer j; $\mathbf{k}_\perp$ is a wave vector along [001]; and $N_\perp$ is the number of impurity planes considered. Finally, the Green's function of the perturbed system G can be derived from G^0 and U following standard scattering theory.[23] The states in the GaAs gap induced by the InAs layer perturbation can be found searching the roots of the secular equation[23]

$$D(E)\equiv\det[\mathbf{1}-G^0(E)U]=0. \tag{2}$$

Due to the basis choice [Eq. (1)], the rank of the secular equation is given by the *number of impurity layers* times the dimension of the ETB orbital basis. Thus, for 1 ML, solving

TABLE II. Transition energies in eV between the HH and the CB1 state induced by 1 ML of InAs in GaAs calculated by the ETB model described in the text and compared with EFA results, a one-dimensional tight-binding model (1DTB), and experimental data.

ETB	1DTB	EFA	Experiments
1.455			1.470,[d] 1.445,[e] 1.488[f]
	1.467[a]		1.473[a]
		1.434[b]	1.430[b]
		1.468[c]	1.468[c]

[a]Reference 1.
[b]Reference 2.
[c]Reference 3.
[d]Reference 4.
[e]Reference 5.
[f]Reference 6.

Eq. (2) consitutes a very modest numerical task. We have used direct matrix inversion to compute G^0. For E in the energy gap of H^0, G^0 is well defined, whereas in the continuum of H^0 a small imaginary part ϵ has been added to E and convergence of the results for $\epsilon \to 0$ has been checked. A numerical precision of 1 meV has been attained. A resonance in the continuum is located at the energy for which $\mathrm{Re}[D(E+i\epsilon)]$ is zero and $\mathrm{Im}[D(E+i\epsilon)]$ has a finite value or, equivalently, where the phase shift is an odd multiple of $\pi/2$. As Eq. (2) depends parametrically on the in-plane wave vector $\mathbf{K}$, the *two-dimensional* dispersion relation $E(\mathbf{K})$ of the bound states is obtained by mapping out the roots of $D(E)$ in $\mathbf{K}$ space. The orbital character of bound and resonant states can be directly obtained from the diagonal elements of G.[20]

III. RESULTS

We have calculated with the above procedure the energy levels and resonances induced by 1 ML of InAs in GaAs. The results for the transition energies from the heavy-hole (HH) to the first electronic state (CB1) are reported in Table II together with some experimental, EFA, and one-dimensional tight-binding results. To our knowledge, a complete theory of excitons for very thin layers has not yet been established. However, since the free-exciton binding energy of the bulk InAs can be estimated to be about 1 meV (Ref. 24) and it has been shown for the $GaAs/Al_xGa_{1-x}As$ system[25] that the exciton binding energy for thin layers can be higher than the two-dimensional limit, we expect that the exciton binding energy in this system be about 5 meV. Excitonic effects have been thus neglected as far as the HH-CB1 transition was concerned. We will briefly discuss in the following the excitonic effects for the LH-CB1 transition. Good overall agreement is found for the HH-CB1 transition compared to the available experimental data. The scattering of the latter can be ascribed to different thicknesses of the nominal 1-ML-InAs sheets. Also, due to the high lattice mismatch between InAs and GaAs, a certain amount of interface roughness and/or alloy formation is likely to be present in this system. These effects change the effective scattering potential induced by the InAs impurity layers, thus affecting the carrier binding energies.

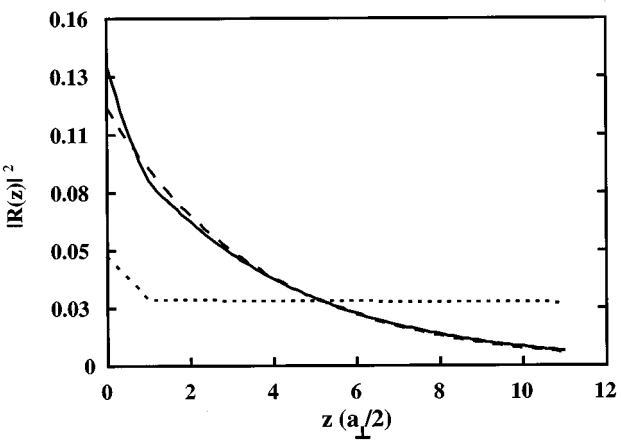

FIG. 1. Carrier probability per fcc monolayer in GaAs with 1 ML of InAs as a function of z (in units of the impurity layer width $a_\perp/2$) at Γ. $a_\perp$ is the interplanar spacing of strained InAs for $z=0$ and the interplane GaAs lattice constant for $z>0$, respectively. The solid line represents the HH bound state, the dashed line the CB1 electron state, and the dotted line the LH resonance.

The EFA results cited in Table II are also in strikingly good agreement with the respective experimental measurements;[2,3] note, however, that the EFA model has adjustable parameters (e.g., quantum-well width), which are usually used to fit to experiment. At the same time, the EFA data are spread considerably due to the sensitivity of this approach to those adjustable parameters. Conversely, the ETB uses parameters fitted to well-known *bulk* values. The only ''free'' parameter are ΔE_v, which can be fixed by independent experimental or *ab initio* results.

It is interesting to note that the HH and the CB1 are localized on the InAs layer with nearly the same weight. Figure 1 shows the probability per fcc monolayer as a function of z at Γ for the HH (solid line) and the CB1 (dashed line). The wave functions have been calculated by solving the usual Lippman-Schwinger equation.[23] The same degree of localization of the HH and CB1 is due partly to the different level deepness in the GaAs gap and partly to the different effective-mass ratio between the HH and the CB1 electron of (strained) InAs and GaAs at the interface. A similar result has been found by Li *et al.*[26] with a tight-binding model describing 1 ML of InAs embedded into 28 layers of GaAs. Even if the bulk effective masses are well reproduced by our model in comparison to the EFA ones (e.g., the HH mass of InAs strained on GaAs is $0.043m_0$ in the ETB model and $0.05m_0$ in the EFA,[27] where m_0 is the free-electron mass), the ETB model predicts a decay length λ of 14 Å, obtained from fitting an exponential decay law $\exp[-x/\lambda]$ to the curves in Fig. 1. In the EFA, $\lambda = 1/\sqrt{m^* E}$ in a.u., with m^* being the *bulk GaAs effective mass* and E the binding energy. We find the HH state 16 meV from the GaAs valence-band edge, whereas the CB1 electron state is located at 49 meV from the GaAs conduction-band edge (the one-dimensional tight-binding model of Ref. 1 predicts a binding energy of 23 meV and 30 meV for the HH and electron, respectively; a CB1 binding energy of 85 meV can be inferred from Ref. 13). In the EFA we thus obtain $\lambda = 21$ Å for the HH and 32 Å for the electron. The strong localization of the HH and the

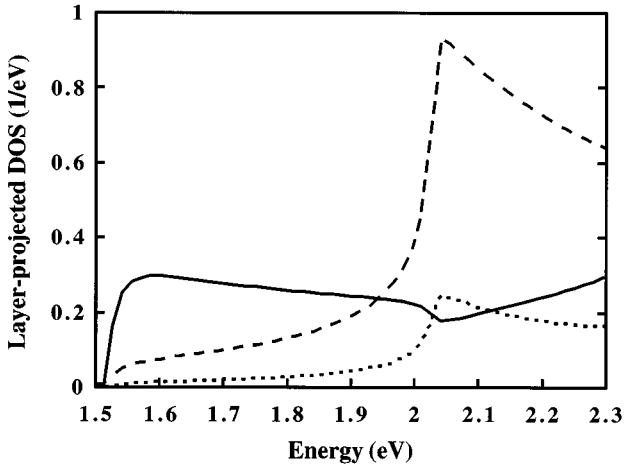

FIG. 2. Conduction-band DOS projected on the InAs layer and resolved into s (solid line), p_z (dashed line), and s^* (dotted line) atomiclike character. The resonance at 1.60 eV has dominant s character and is thus a Γ_6-derived state. The second resonance at 2.03 eV has p_z and s^* character and is the GaAs projected X_6 state.

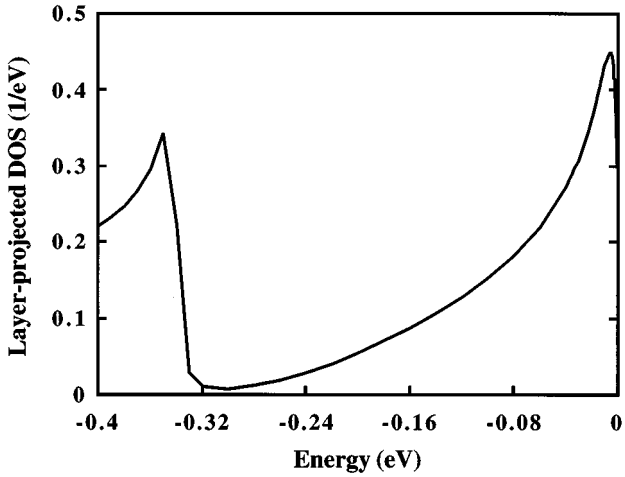

FIG. 3. Valence-band DOS projected on the InAs layer and resolved into p_z atomiclike character (the s and s^* components being negligible). The peak at -7 meV corresponds to a resonance located at -3 meV (see the text). The second peak at about -0.34 meV is the split-off GaAs projected state.

electron explains the high recombination efficiency usually observed in this system.[7]

A resonance is found in the conduction band at 1.60 eV. By calculating the DOS projected on the InAs layer and resolving it into its atomic-orbital components it becomes clear that, due to its s character, it is a Γ_6-derived state (see Fig. 2). This resonance corresponds to the first resonant state in a one-dimensional EFA model. It is not evident at present if this state can contribute to the absorption. The second resonance at 2.03 eV has dominant p_z and s^* character and an ''antiresonance'' s one and is the GaAs projected X_6-derived state. We stress that this resonance *cannot* be reproduced at Γ by the EFA since it is the result of the mixing of all states along the [001] direction of the GaAs three-dimensional BZ.

In the EFA the LH state is evidently bound since a one-dimensional attractive potential always binds a state in a one-band model irrespective of the strength of the potential. Conversely, our model predicts no LH state in the GaAs gap. In the present approach, for each **K** the system is mapped into an effective one-dimensional chain problem.[13] However, its multiband character is retained and different one-dimensional bands interact. Thus, in this model, an attractive potential always binds one state (corresponding to the HH state), but *not* necessarily a second one (i.e., the LH). Thus a nearly unbound state at Γ in a one-band EFA theory (the EFA predicts a LH binding energy of $+1$ meV) can be completely unbound in the ETB model if all states in the BZ are correctly included in the diagonalization of H. In fact, we found that the LH is degenerate with the continuum at about 3 meV below the GaAs valence-band edge. Its probability per fcc monolayer as a function of z at Γ is shown in Fig. 1 (dotted line). Since the state belongs to the continuum an arbitrary normalization factor has been used to put it on a common scale with the CB1 and HH bound states. It is evident that a hole in this state is delocalized into the GaAs barriers, but has a certain probability to be found on the InAs layer. The p_z component of the layer-projected DOS near the zero of energy (the s and s^* components being negligible) is plotted in Fig. 3. The DOS presents a peak at -7 meV. It is shifted with respect to the location of the resonance due to the strong energy dependence (like $1/\sqrt{E}$ for $E\rightarrow 0$) of the unperturbed GaAs DOS.[23] The peak at about -0.34 eV is the GaAs split-off band projected DOS. The role of strain in determining the resonance character of the LH is easily seen. The uniaxial strain in InAs splits the degenerate valence-band manifold and pushes the HH state (with symmetry p_x, p_y) upward in energy relative the average energy of the manifold. Conversely, the strain pushes the LH state (with symmetry p_z) downward, thus adding a *repulsive* component to the impurity potential. This statement is illustrated in Fig. 4, where the [10] in-plane dispersions of the HH and LH of InAs and GaAs are plotted on a common energy scale (i.e.,

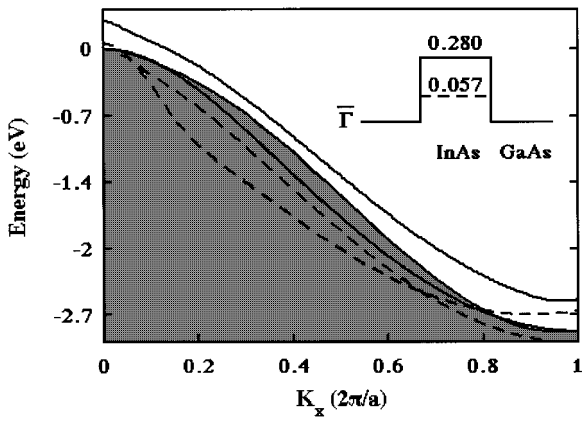

FIG. 4. HH (solid line) and LH (dashed line) dispersions in the [10] in-plane direction for InAs and GaAs. The shaded region represents the continuum of the (001) layer-projected GaAs bulk bands. A crossover from the bound to the resonant state in the LH dispersion is evident at $\mathbf{K}_x \approx 0.06(2\pi/a)$ (a is the in-plane GaAs lattice constant). The inset shows the Γ HH and LH offset profiles in the z direction (not in scale). The zero of energy is the GaAs valence-band edge.

the HH and LH offsets have been added to the InAs energies at Γ; see the inset). The continuum generated by the (001) layer-projected GaAs bulk bands is shaded. A crossover from ''type-I'' to ''type-II'' band alignment of the InAs LH dispersion appears at $\mathbf{K}_x \approx 0.06(2\pi/a)$ (a is the in-plane GaAs lattice constant). The type-I alignment is restored at $\mathbf{K}_x \approx 0.7(2\pi/a)$. This means that the LH is pushed into the continuum by strain throughout the majority of the two-dimensional BZ and the effective LH offset of 57 meV between GaAs and InAs is not sufficient to bind a state at Γ. These results would thus suggest a type-II LH exciton formed by the electron bound by the InAs layer and the hole in the GaAs barriers. Conversely, the EFA would predict a type-I configuration since the LH offset corresponds to an attractive one-dimensional potential.

Due to the very low degeneracy of the LH state with the continuum (3 meV) we suggest that absorption or temperature-dependent luminescence[28] experiments can distinguish between a bound or an unbound LH state. In fact, if the LH state is unbound, as it is predicted by our model, at very low temperatures only the HH-CB1 transition should be detected (in an ideal defect-free sample). Increasing the temperature, the type-II transition between the GaAs hole state and the CB1 should become visible. Increasing further the temperature of 3 meV should reveal a luminescence peak coming from the LH resonance and the CB1 transition. All these considerations are valid if one assumes the same lifetime for the above recombination processes and low charge transfer from the LH resonance and the valence-band top of the GaAs barriers (due to nonradiative acoustic-phonon scattering).

Finally, we stress that our model completely neglects the electron-hole Coulomb interaction. It is not clear at present which is the role of the latter on the LH resonance exciton. The luminescence results of Refs. 1,2 and 5 seem to indicate that a very shallow *exciton* state is bound in this system. According to our picture, this means that the electron-hole *final-state* interaction should provide at least a binding energy of 3 meV. A complete theory of the LH-derived exciton for very thin layers should clarify this point. Some work in this direction is thus in order.

IV. CONCLUSION

We have studied in detail the electronic properties of 1 ML of InAs in GaAs with an ETB model. Our main results can be summarized as follows. (i) The predicted HH-CB1 transition is in good agreement with the EFA and experimental data. (ii) We predict a Γ_6-derived and an X_6-derived conduction-band resonance, respectively. The first one is an EFA-like state. The second one is the GaAs-projected X_6 state and is due to the mixing of all states along the [001] direction of the GaAs three-dimensional BZ. (iii) As far as the valence-band is concerned, we find a HH state bound at 16 meV above and a LH state degenerate with the continuum 3 meV below the GaAs valence-band edge. The latter finding is in *disagreement* with an EFA picture and suggests a type-II LH-CB1 exciton in this system. The strain plays an important role in determining this energy-level order since it pushes the LH into the continuum even if the LH offset between (strained) InAs and GaAs at Γ corresponds to an attractive potential for the LH. We suggest that, due to the low LH state degeneracy with the continuum, absorption or temperature-dependent luminescence measurements could distinguish between a bound or an unbound LH state. Further investigation of this point is thus necessary. In particular, a complete exciton theory for very thin layers is needed that goes beyond both the EFA and the single-particle picture of the present ETB model.

ACKNOWLEDGMENT

We acknowledge A. Bitz for useful discussions.

APPENDIX: EMPIRICAL TIGHT-BINDING MODEL

1. Spin-orbit interaction

We start from the empirical tight-binding Hamiltonian of Vogl *et al.*,[19] which is written in the block form

$$H^0 = \begin{pmatrix} h_{aa} & h_{ac} \\ h_{ca} & h_{cc} \end{pmatrix}, \quad h_{ca} = h_{ac}^{\dagger}. \tag{A1}$$

In the sp^3s^* basis the individual blocks have dimension 5×5 and the subscripts a and c denote the anion and cation, respectively.

The spin-orbit interaction is incorporated in the ETB Hamiltonian following the prescription of Chadi[31] for tight-binding Hamiltonians. Starting from the free-atom spin-orbit splitting, Chadi uses renormalized values in the solid, which are chosen such as to reproduce the observed splittings at Γ. In the zinc-blende lattice two distinct spin-orbit parameters are needed and only on-site matrix elements of the spin-orbit interaction H^{so} are nonzero. In the sp^3s^* model only the p orbitals contribute and we use the following definitions of the parameters:

$$\begin{aligned} \langle xb\uparrow | H^{\mathrm{so}} | zb\downarrow \rangle &= \lambda_b, \\ \langle yb\uparrow | H^{\mathrm{so}} | zb\downarrow \rangle &= i\lambda_b, \\ \langle xb\uparrow | H^{\mathrm{so}} | yb\uparrow \rangle &= i\lambda_b, \end{aligned} \tag{A2}$$

where $b = a, c$ denotes the ion type, $\lambda_a = \frac{1}{3}\Delta_a$, $\lambda_c = \frac{1}{3}\Delta_c$, and Δ_b are the ''renormalized'' atomic spin-orbit splittings.[31] The remaining matrix elements are either zero or related to the ones given above by noting that the $\downarrow\downarrow$ submatrix is the *complex conjugate* of the $\uparrow\uparrow$ submatrix and the $\downarrow\uparrow$ submatrix the *Hermitian conjugate* of the $\uparrow\downarrow$ one. λ_a and λ_c are given in Table I.

2. The perturbation matrix U

The perturbation U is assumed to affect the on-site and nearest-neighbor matrix elements at the substitutional sites. To find the representation of U in the layer-orbital basis $|\mathbf{K}lj\rangle$ we exploit our knowledge of the matrix elements in $\mathbf{k}$ space and do a one-dimensional Fourier transform

$$\langle \mathbf{K}lj|U|\mathbf{K}l'j'\rangle = \frac{1}{N_\perp}\sum_{\mathbf{k}_\perp} e^{-i\mathbf{k}_\perp(\mathbf{R}_{j'}-\mathbf{R}_j)} \times\langle \mathbf{K}+\mathbf{k}_\perp, lb|U|\mathbf{K}+\mathbf{k}_\perp, l'b'\rangle, \quad -n\leqslant j,j'\leqslant n, |j-j'|\leqslant 1. \tag{A3}$$

b,b' denote the ion types of layers j,j', respectively. $U(\mathbf{k})=H^I(\mathbf{k})-H^0(\mathbf{k})$, where H^I is the Hamiltonian of the (strained) interlayer *bulk material* with eigenvalues shifted by the valence band offset $\Delta\overline{E_v}$.

The submatrices $U_{jj'}$ have a structure similar to that of the blocks $h_{bb'}$ in H^0 in Eq. (A1). The blocks $j=j'$ are diagonal with matrix elements $\Delta E(l,b(j))$ and those in the off diagonals $|j-j'|=1$ represent either anion-cation or cation-anion interactions. Using $U_{j,j\pm1}=U^\dagger_{j\pm1,j}$ and the recurrence property $U_{j+2,j'+2}=U_{jj'}$, the perturbation matrix is easily built for arbitrary interlayer thickness. As an example, we give the block form of a single-monolayer impurity, i.e.,

$$U=\begin{pmatrix} \widetilde{U}_{-1-1} & U_{-10} & 0 \\ U_{0-1} & U_{00} & U_{01} \\ 0 & U_{10} & \widetilde{U}_{11} \end{pmatrix}. \tag{A4}$$

The common-ion submatrices at the interlayer boundary $\widetilde{U}_{11}$ and $\widetilde{U}_{-1-1}$ are scaled by a factor 1/2, as explained in Sec. II. The extension to the spin-orbit-dependent case is straightforward by virtue of Eq. (A2), whereby the dimensions of the $U_{jj'}$ submatrices are doubled.

3. Inclusion of strain

In order to reproduce the effects of strain on the InAs bulk bands we proceeded in the following way. We scaled the Koster-Slater two-center integrals with the usual power law[29]

$$v_\alpha = v^0_\alpha\left(\frac{d}{d_0}\right)^{-n_\alpha}, \tag{A5}$$

where α denotes the type of two-center integral[18] and d_0 and d are the equilibrium and distorted bond lengths, respectively. We found the deformation potential $a=-6.2$ eV [to be compared to the experimental value $a=-6$ eV (Ref. 24)] with $n_{ss}=3.54$ and the other $n_\alpha=2$. The deformation potential b has been fitted considering the changes of the crystal-field interactions due to the uniaxial stress. The energy parameters $E(p,b)$ have been changed according to the law[30]

$$\begin{aligned} E(p,b)_{x,y} &= E(p,b)+b_p(\epsilon_{xx}-\epsilon_{zz}), \\ E(p,b)_z &= E(p,b)-2b_p(\epsilon_{xx}-\epsilon_{zz}), \end{aligned} \tag{A6}$$

where ϵ_{xx} and ϵ_{zz} are the in-plane and interplane strain components, respectively, and b_p is a constant to be fitted in order to reproduce the deformation potantial b. We found $b=-1.8$ eV [the experimental value is $b=-1.8$ eV (Ref. 24)], with $b_p=0.7$.

[1] R. Cingolani, O. Brandt, L. Tapfer, G. Scamarcio, G. C. La Rocca, and K. Ploog, Phys. Rev. B **42**, 3209 (1990).

[2] O. Brandt, L. Tapfer, R. Cingolani, K. Ploog, M. Hohenstein, and F. Phillipp, Phys. Rev. B **41**, 12 599 (1990).

[3] J. H. Lee, K. Y. Hsieh, and R. M. Kolbas, Phys. Rev. B **41**, 7678 (1990).

[4] O. Brandt, H. Lage, and K. Ploog, Phys. Rev. B **43**, 14 285 (1991).

[5] O. Brandt, H. Lage, and K. Ploog, Phys. Rev. B **45**, 4217 (1992).

[6] M. I. Alonso, M. Ilg, and K. H. Ploog, Phys. Rev. B **50**, 1628 (1994).

[7] R. Schwabe, F. Pietag, M. Faulkner, S. Lassen, V. Gottschalch, R. Franzheld, A. Bitz, and J. L. Staehli, J. Appl. Phys. **77**, 6295 (1995).

[8] R. Colombelli, J. M. Jancu, F. Beltram, L. Sorba, D. Bertho, and C. Jouanin, Appl. Phys. Lett. **68**, 1534 (1996).

[9] J. E. Bernard and A. Zunger, Appl. Phys. Lett. **65**, 165 (1994).

[10] K. A. Mäder and A. Zunger, Phys. Rev. B **50**, 17 393 (1994).

[11] A. Franceschetti and A. Zunger, Phys. Rev. B **52**, 14 664 (1995).

[12] H. P. Hjalmarson, J. Vac. Sci. Technol. **21**, 524 (1982)

[13] S. Wilke and D. Hennig, Phys. Rev. B **43**, 12 470 (1991).

[14] K. A. Mäder and A. Baldereschi, in *Proceedings of the International Meeting on the Optics of Exitons in Confined Systems*, edited by A. D'Andrea, R. Del Sole, R. Girlanda, and A. Quattropani (Institute of Physics, Bristol, 1992), p. 341; K. A. Mäder and A. Baldereschi, in *Advanced III-IV Compound Semiconductor Growth, Processing and Devices*, edited by S. J. Pearton, D. K. Sadana, and I. M. Zavada, MRS Symposia Proceedings No. 240 (Materials Research Society, Pittsburgh, 1992), p. 597.

[15] A. Bitz, C. Jordan, M. Di Ventra, K. A. Mäder, L. C. Andreani, J. F. Carlin, A. Rudra, and J. L. Staehli, Nuovo Cimento D **17**, 1367 (1995).

[16] J. W. Matthews, in *Epitaxial Growth*, edited by J. W. Matthews (Academic, New York, 1982), p. 563.

[17] A. Patanè, A. Polimeni, M. Capizzi, F. Martelli, L. Lazzarini, G. Salviati, and L. Nasi, in *Proceedings of the 23rd International Conference on the Physics of Semiconductors*, edited by M. Scheffler and R. Zimmermann (World Scientific, Singapore, 1996), p. 1305.

[18] G. F. Koster and J. C. Slater, Phys. Rev. **96**, 1208 (1954).

[19] P. Vogl, H. P. Hjalmarson, and J. D. Dow, Phys. Chem. Solids **44**, 365 (1983).

[20] Note, however, that using an *ad hoc* s^* orbital to mimic the effect of d orbitals on the band structure can produce misleading s-like *character* of certain conduction states.

[21] J. C. Woicik, J. G. Pellegrino, S. H. Southworth, P. S. Shaw, B. A. Karlin, C. E. Bouldin, and K. E. Miyano, Phys. Rev. B, **52**, R2281 (1995).

[22] N. Tit, M. Peressi, and S. Baroni, Phys. Rev. B **48**, 17 607 (1993).

[23] E. N. Economou, *Green's Functions in Quantum Physics* (Springer, Berlin, 1979).

[24] *Numerical Data and Functional Relationships in Science and Technology*, edited by O. Madelung and M. Schulz, Landolt-Börnstein, New Series, Group III, Vol. 22, Pt. a (Springer, New York, 1987).

[25] L. C. Andreani and A. Pasquarello, Phys. Rev. B **42**, 8928 (1990).

[26] G. H. Li, A. R. Goñi, C. Abraham, K. Syassen, P. V. Santos, A. Cantarero, O. Brandt, and K. Ploog, Phys. Rev. B **50**, 1575 (1994).
[27] R. People and S. K. Sputz, Phys. Rev. B **41**, 8431 (1990).
[28] L. P. Fu, F. T. Bacalzo, G. D. Gilliland, R. Chen, K. K. Bajaj, and J. Klem, Phys. Rev. B **51**, 17 630 (1995).
[29] C. Priester, G. Allan, and M. Lannoo, Phys. Rev. B **37**, 8519 (1988).
[30] G. Grosso and C. Piermarocchi, Phys. Rev. B **51**, 16 772 (1995).
[31] D. J. Chadi, Phys. Rev. B **16**, 790 (1977).